

Assignment 3

1. Description of Adjoint Weighted Residual

We can use the method of Adjoint Weighted Residuals (AWR) to figure out the impact of the residual errors on the functionals we are interested in evaluating. When we can compute the impact of this residual error on a finer space solution, we can incorporate this information and get an improvement on the functionals we evaluated using a much coarser space. The procedure is explained below:

- Generate a coarse mesh space \mathcal{M}_H with polynomial interpolation of order p_H . Solve for the state variables q_H on this space such that $\mathcal{R}_H(q_H) < 10^{-12}$.
- Use the coarse space solution to find the functional $J_H(q_H)$.
- Now generate a fine space mesh \mathcal{M}_h using only p -enrichment, where the number of elements n_e remains fixed, but a higher order polynomial $p_h > p_H$, is used to interpolate between the solutions.
- We use a prolongation operator I_h^H such that $I_h^H q_h = q_h^H$ and prolong the coarse space solution to find an approximation of how it will be on a finer mesh \mathcal{M}_h .
- Now, there are a couple of ways to proceed:
 - (a) **Prolongation of coarse space solution q_H to a fine space q_h^H**
 - i. We then find the fine-space functional J_h using the prolonged solution q_h^H , $J_h(q_h^H)$.
 - ii. We then use the same prolonged solution q_h^H to find the residual errors on the fine space mesh \mathcal{M}_h , $\mathcal{R}_h(q_h^H)$.
 - iii. After finding the residual error on \mathcal{M}_h with q_h^H , we find the adjoints

$$\psi_h = - \left(\frac{\partial \mathcal{R}_h}{\partial q_h^H} \right)^{-T} \frac{\partial J_h}{\partial q_h^H}.$$

(b) Patch based reconstruction

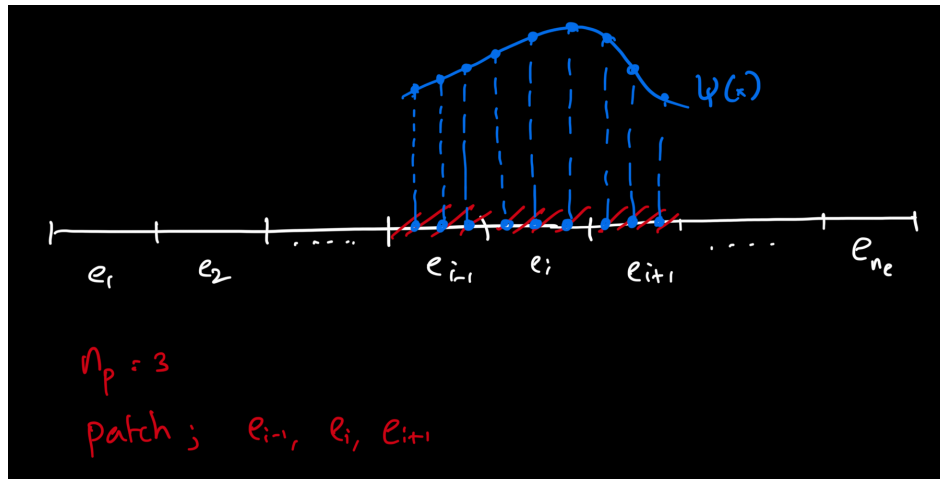


Figure 1: Patching 3 elements and interpolating the solutions

- i. We solve for the adjoint variables ψ_H on \mathcal{M}_H using q_H .
- ii. Then we use a patch based reconstruction shown in Fig 1, where neighboring elements are patched together (n_{patch}) in \mathcal{M}_H and the nodal solutions in the patched elements are interpolated using a polynomial of degree $p_{\text{patch}} = p_h + 1$.

$$V = \begin{bmatrix} 1 & x_H[j, e_p] & \dots & x_H[j, e_p]^{p_{\text{patch}}} \end{bmatrix},$$

$$f = [\psi_H[1, 1] \dots \psi_H[n_{\text{sbp}}^H, n_{\text{patch}}]]^T,$$

where $j = [1, n_{\text{sbp}}^H]$ and $e_p = 1, \dots, n_{\text{patch}}$. n_{sbp}^H is the number of sbp nodes in \mathcal{M}_H elements. V is the Vandermonde matrix and r is the value of the adjoints at the coarse space \mathcal{M}_H . This Least Squares problem is solved and the polynomial coefficients are found,

$$c_h = (V^T V)^{-1} V^T f.$$

- iii. We use these coefficients to interpolate and find the fine-space adjoints ψ_h at sbp node j and element e as,

$$\psi_h[j, e] = \sum_{k=0}^{p_{\text{patch}}} c_h^k x_h[j, e]^k.$$

- iv. We then use the same prolonged solution q_h^H to find the residual errors on the fine space mesh \mathcal{M}_h , $\mathcal{R}_h(q_h^H)$.

- The True error is given by,

$$\text{err}_{\text{true}} = |J_{\text{ex}} - J_H|.$$

- The Estimated error is given by,

$$\text{err}_{\text{est}} = |J_H - J_h(q_h^H) - \psi_h^T \mathcal{R}_h(q_h^H)|.$$

- The fine-space corrected error is given by,

$$\text{err}_{\text{corr}} = |J_h(q_h^H) + \psi_h^T \mathcal{R}_h(q_h^H) - J_{\text{ex}}|.$$

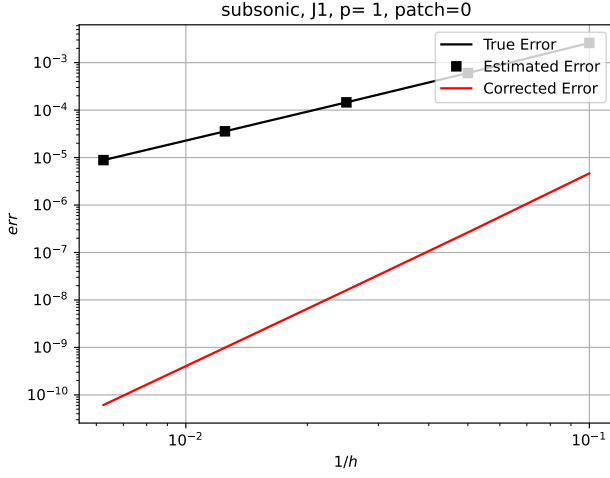
- The effectivity is defined as,

$$\eta = \frac{\text{err}_{\text{est}}}{\text{err}_{\text{true}}}.$$

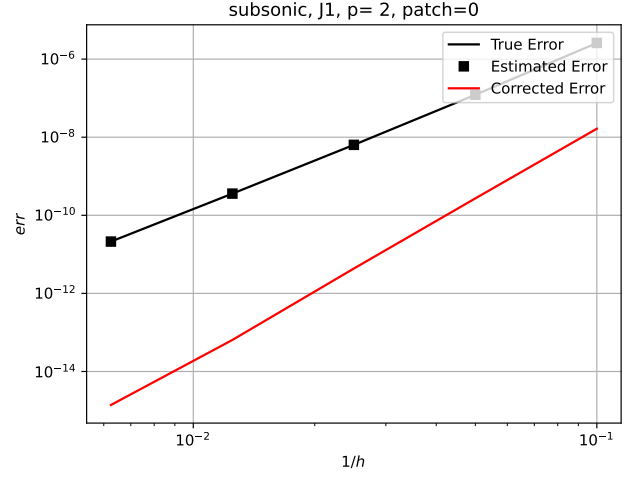
2. Applying AWR to both J_1 , and J_2 for the subsonic nozzle flow.

- (a) Mesh convergence study functionals J_1, J_2 is in Fig 2 and Fig 3 respectively. The effectivity of this method is shown in Fig 4 and Fig 5 for functionals J_1, J_2 respectively. With effectivity $\eta \rightarrow 1$, we can see that AWR is able to help us compute a more accurate functional in spite of using only a coarse mesh \mathcal{M}_H and without requiring the fine space solution q_h . Although we require a fine space adjoint ψ_h , we work around it using the p - enrichment technique or a patch based reconstruction and the results are shown in Fig A.1-Fig A.4 for the mesh convergences and effectivities.

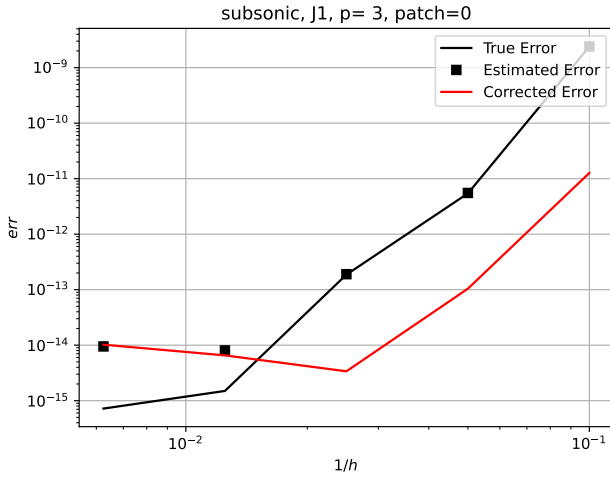
For the cases $p_H = 3, 4$, we can notice that the estimated error no longer matches with the true error and that is because we are in the order of $\varepsilon_{\text{mach}}$.



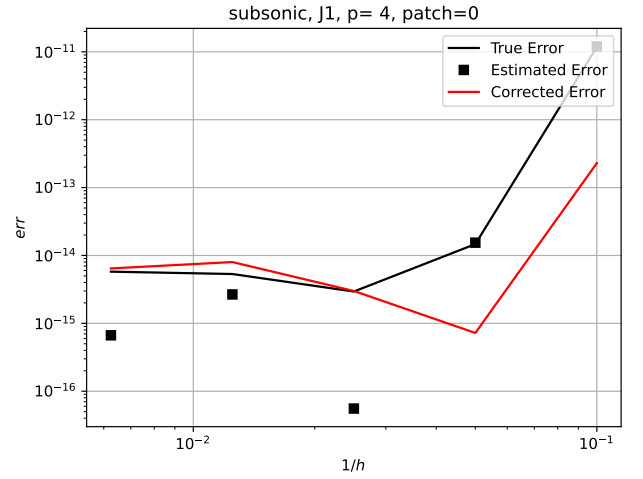
(a) Error convergence with $p_H = 1$ on \mathcal{M}_H for J_1



(b) Error convergence with $p_H = 2$ on \mathcal{M}_H for J_1

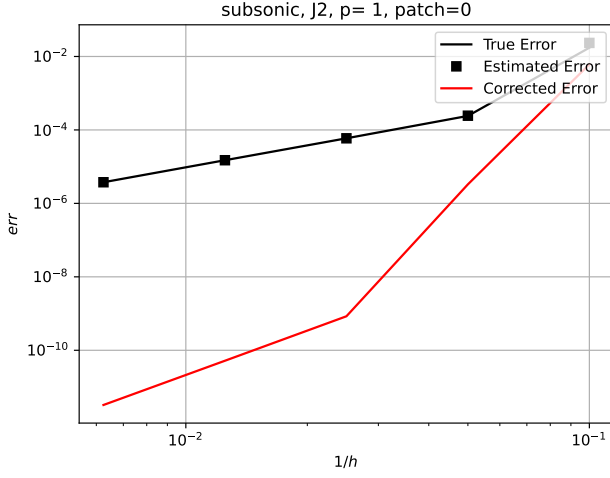


(c) Error convergence with $p_H = 3$ on \mathcal{M}_H for J_1

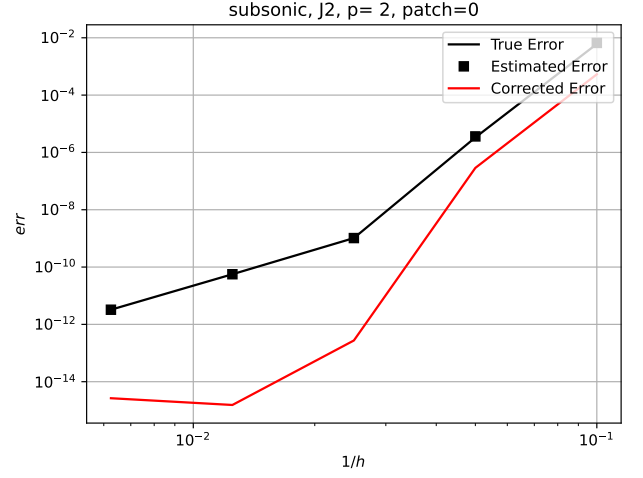


(d) Error convergence with $p_H = 4$ on \mathcal{M}_H for J_1

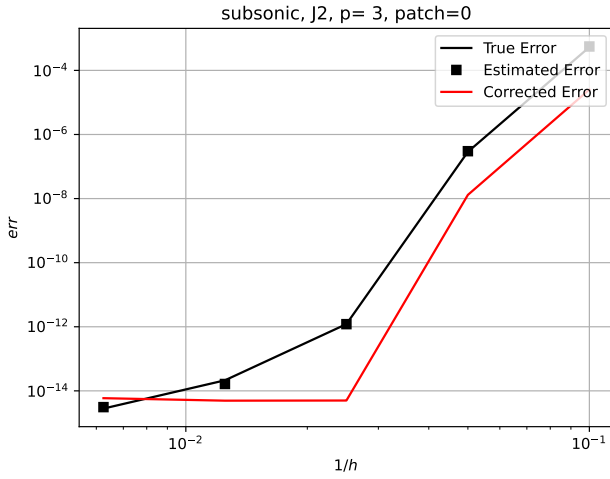
Figure 2: Mesh convergence analysis for functional J_1 using AWR showing the true error, estimated error and the corrected error in the subsonic flow regime.



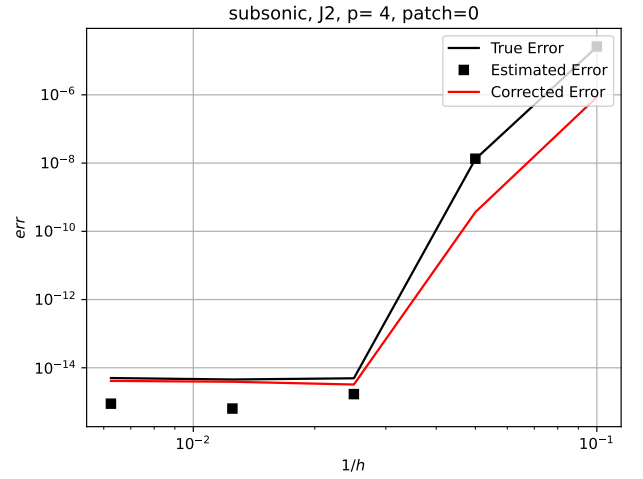
(a) Error convergence with $p_H = 1$ on \mathcal{M}_H for J_2



(b) Error convergence with $p_H = 2$ on \mathcal{M}_H for J_2

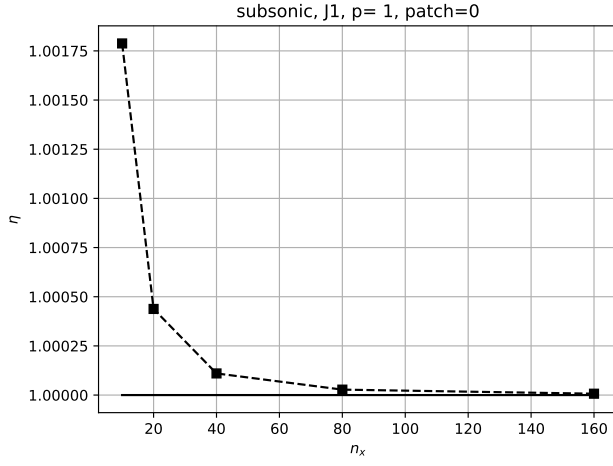


(c) Error convergence with $p_H = 3$ on \mathcal{M}_H for J_2

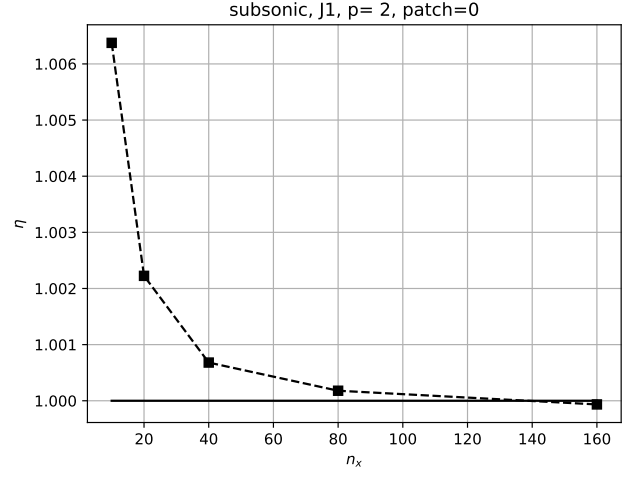


(d) Error convergence with $p_H = 4$ on \mathcal{M}_H for J_2

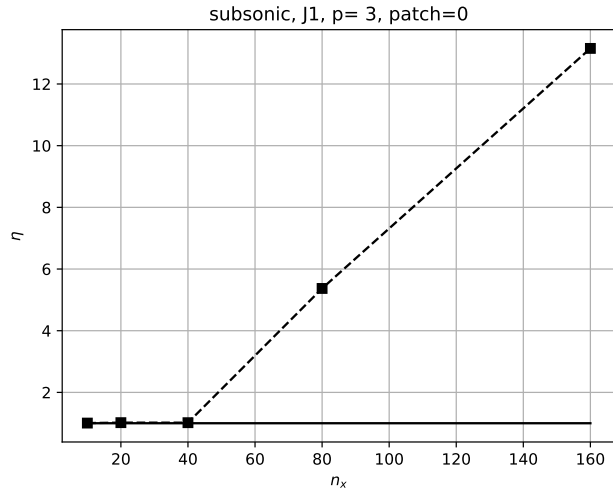
Figure 3: Mesh convergence analysis for functional J_2 using AWR showing the true error, estimated error and the corrected error in the subsonic flow regime.



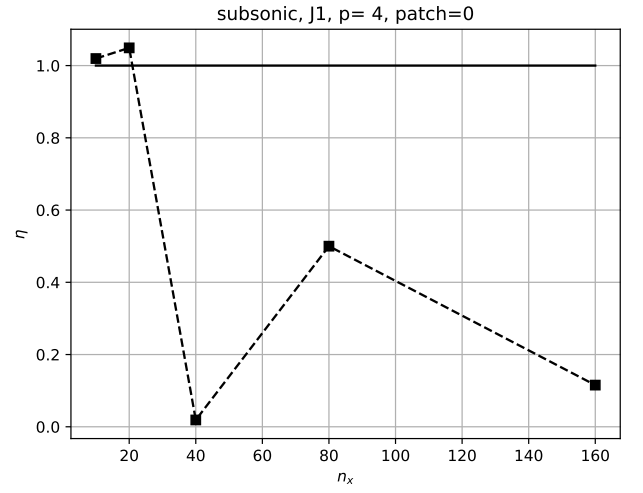
(a) Effectivity with $p_H = 1$ on \mathcal{M}_H for J_1



(b) Effectivity with $p_H = 1$ on \mathcal{M}_H for J_1

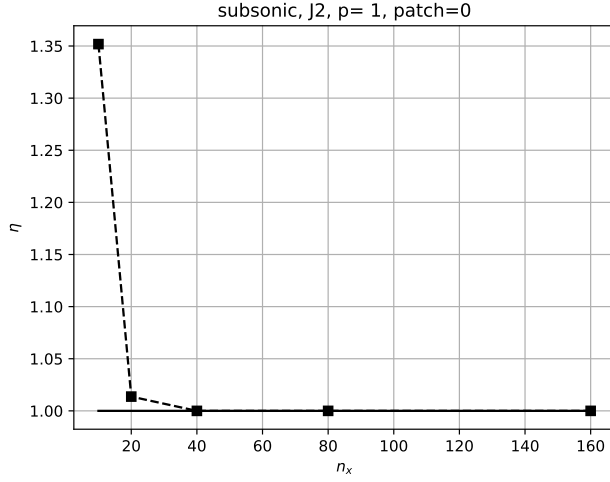


(c) Effectivity with $p_H = 1$ on \mathcal{M}_H for J_1

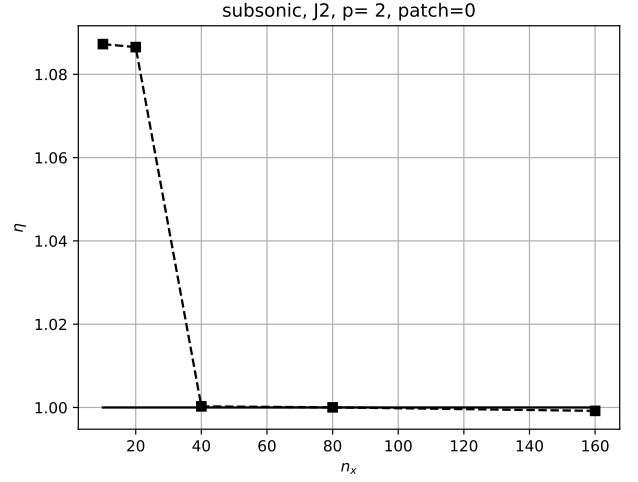


(d) Effectivity with $p_H = 1$ on \mathcal{M}_H for J_1

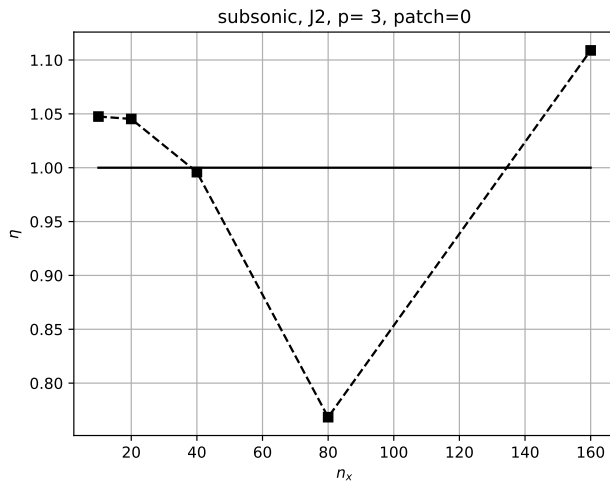
Figure 4: Effectivity for J_1 in the subsonic flow regime.



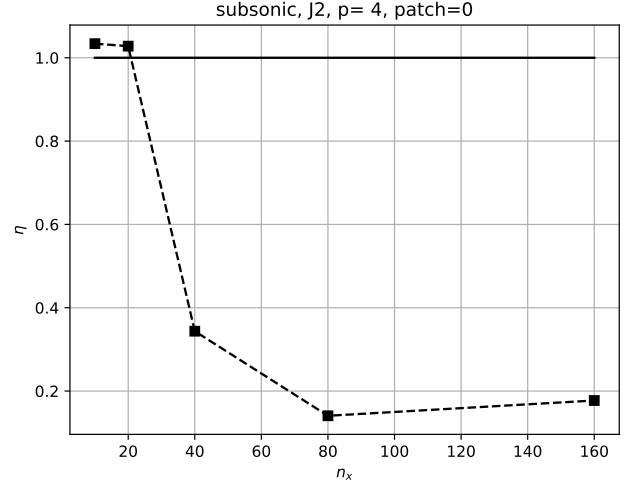
(a) Effectivity with $p_H = 1$ on \mathcal{M}_H for J_2



(b) Effectivity with $p_H = 1$ on \mathcal{M}_H for J_2



(c) Effectivity with $p_H = 1$ on \mathcal{M}_H for J_2



(d) Effectivity with $p_H = 1$ on \mathcal{M}_H for J_2

Figure 5: Effectivity for J_2 in the subsonic flow regime.

- (b) Using AWR to find out where more mesh convergence is required to capture and further reduce residual errors

This study reveals that the adjoint weighted residual errors localized to the elements decrease as the order of the interpolating polynomial is increased from $p_H = 1$ to $p_H = 2$. In order to capture J_1 and J_2 accurately, we need to either do a mesh refinement or increase the polynomial interpolation order to slowly reduce the localized adjoint weighted residual errors. This can be seen in Fig 6 and Fig 7.

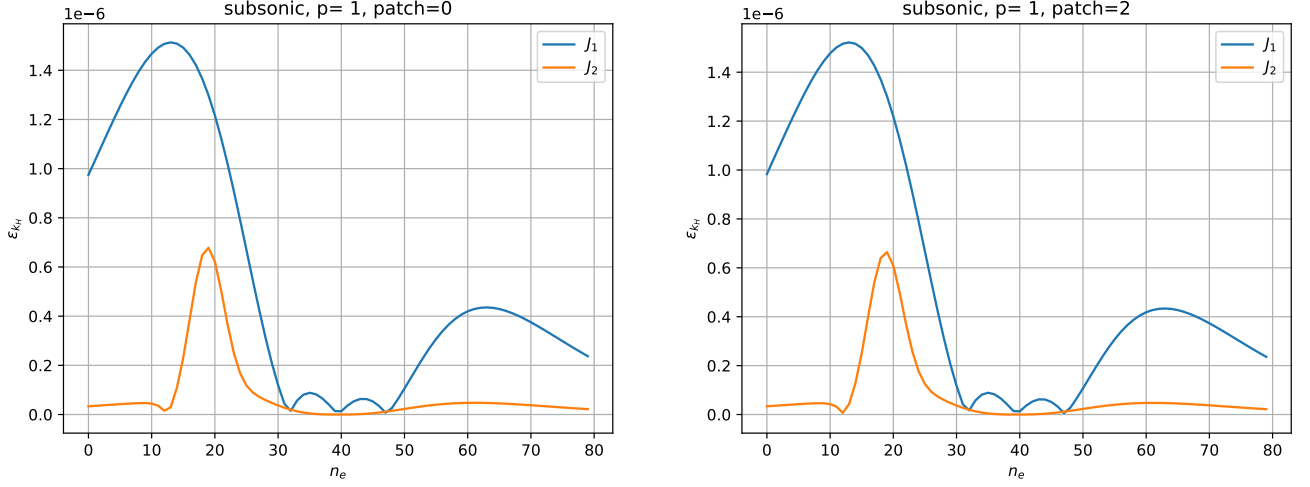


Figure 6: AWR based mesh-refinement study in the subsonic regime for $p_H = 1$.

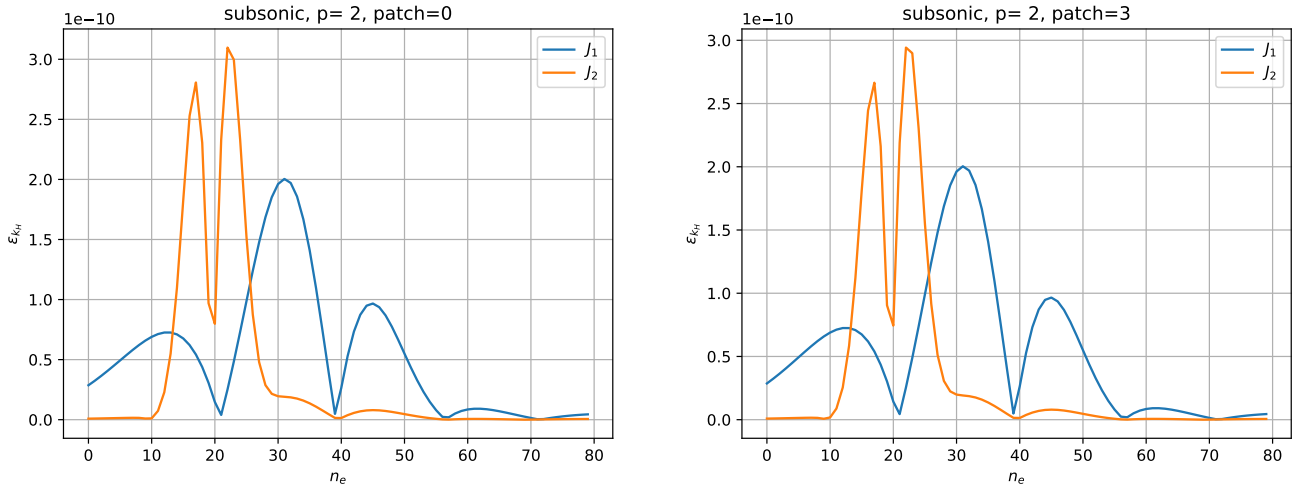
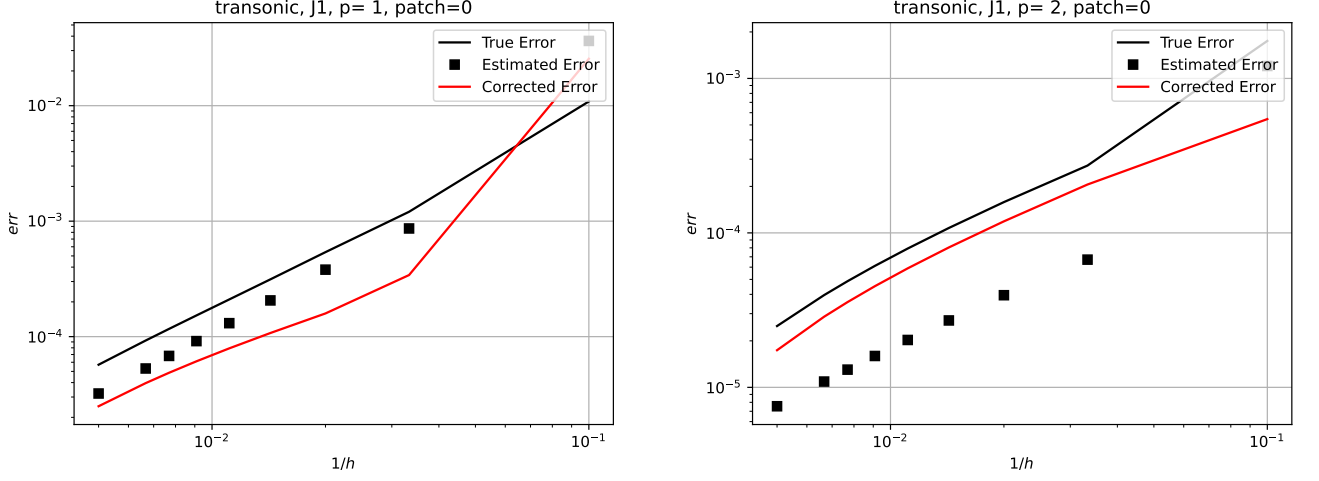


Figure 7: AWR based mesh-refinement study in the subsonic regime for $p_H = 2$.

3. Applying AWR to both J_1 and J_2 for the transonic nozzle flow with a shock at $x = 0.7$

- (a) Mesh convergence analysis shows that the corrected error is actually converging at a similar rate compared to the true error in Fig 8 and Fig 9. The estimated errors are an order of magnitude lower than the true error. This is an indication that due to the shock and nonlinearity in the solutions, p -enrichment is not able to provide any advantage in improving the order of convergence of the corrected error. This is also reflected in the effectivities in Fig 10 and Fig 11 as they are significantly less than 1.0.



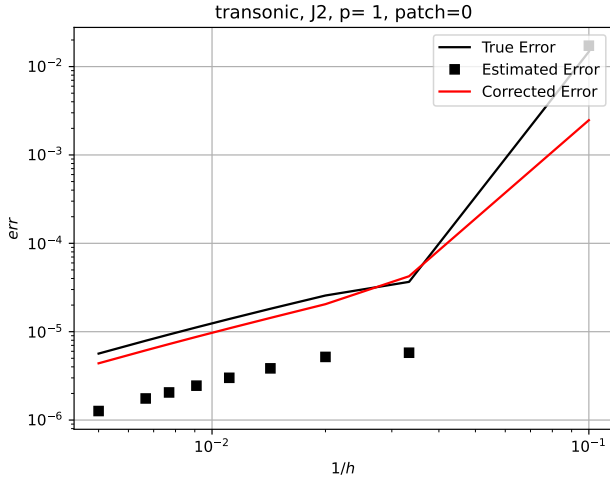
(a) Error convergence with $p_H = 1$ on \mathcal{M}_H for J_1

(b) Error convergence with $p_H = 2$ on \mathcal{M}_H for J_1

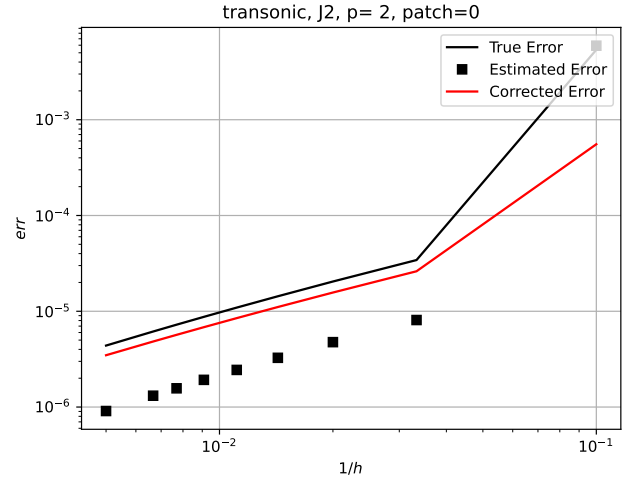
Figure 8: Mesh convergence analysis for functional J_1 using AWR showing the true error, estimated error and the corrected error in the transonic flow regime.

- (b) [Using AWR to find out where more mesh convergence is required to capture and further reduce residual errors](#)

Unlike the subsonic case, AWR provides very important information to isolate where the residual errors are very high and where mesh refinement is absolutely necessary in order to calculate accurate functionals. In Fig 12, since the order of polynomial interpolation is not good enough to numerically capture the nonlinearity in the shock, we can see that AWR suggests we need to refine more at the throat $x = 0.5$ of the nozzle in order to get more accurate adjoints (black curve on Fig 12b) that can weight the residual errors coming from the area of the shock. When a higher degree polynomial order $p_H = 2$ is used, the shock nonlinearity is better captured and AWR from Fig 13 suggests that in order to get better estimates of the functionals, we need to refine near the shock region at $x = 0.7$ to get better q_h . I do not understand the behavior of J_2 in the transonic case and wish to learn that better at a later time.

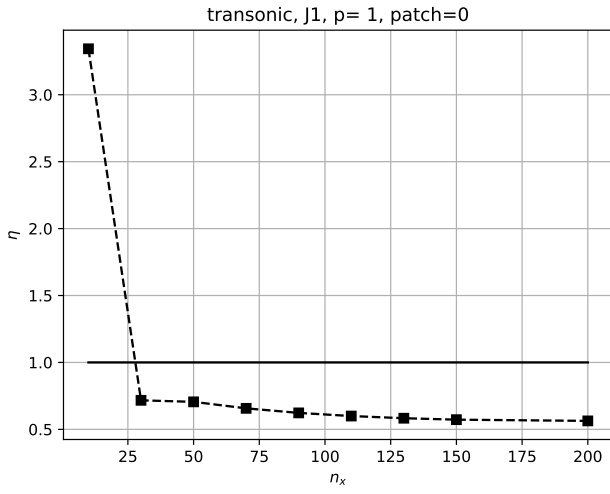


(a) Error convergence with $p_H = 1$ on \mathcal{M}_H for J_2

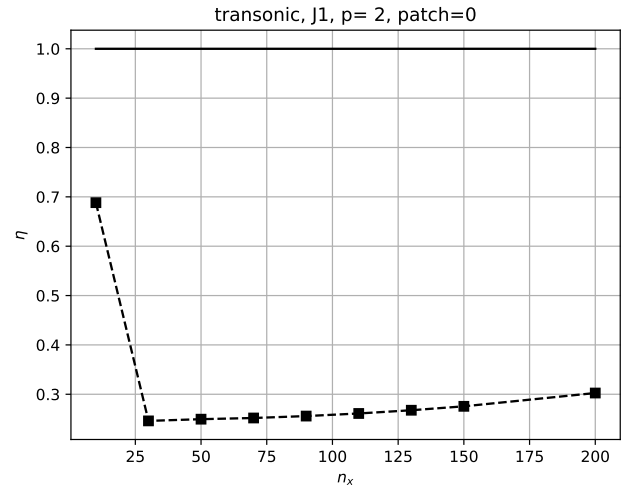


(b) Error convergence with $p_H = 2$ on \mathcal{M}_H for J_2

Figure 9: Mesh convergence analysis for functional J_2 using AWR showing the true error, estimated error and the corrected error in the transonic flow regime.

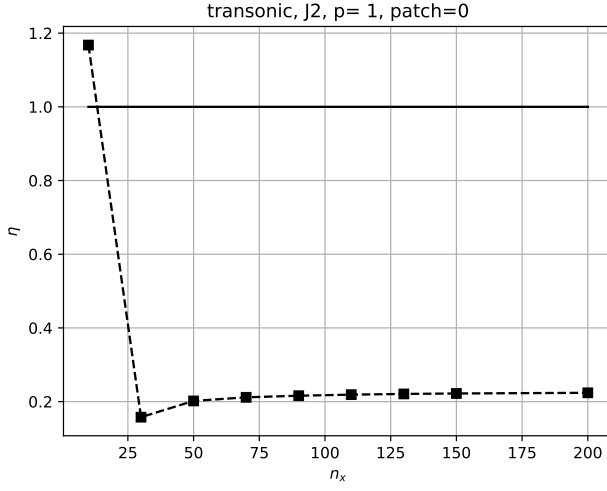


(a) Effectivity with $p_H = 1$ on \mathcal{M}_H for J_1

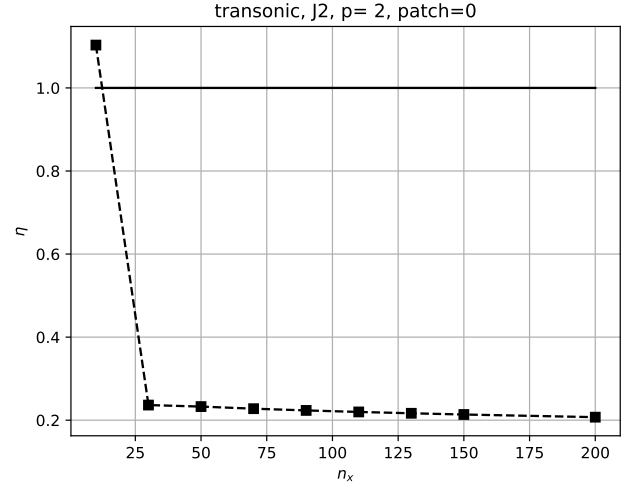


(b) Effectivity with $p_H = 2$ on \mathcal{M}_H for J_1

Figure 10: Effectivity for J_1 in the transonic regime.

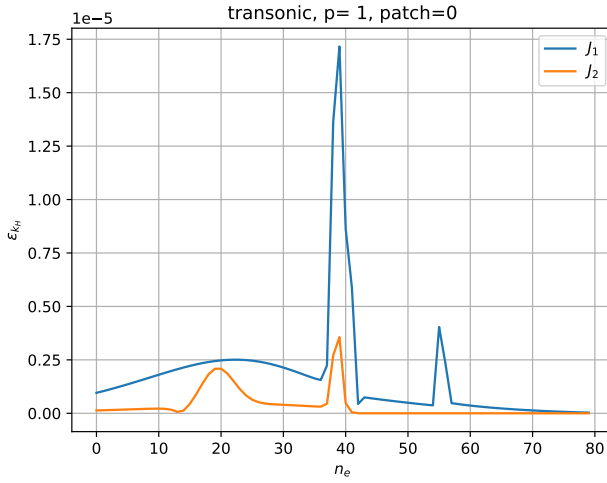


(a) Effectivity with $p_H = 1$ on \mathcal{M}_H for J_2

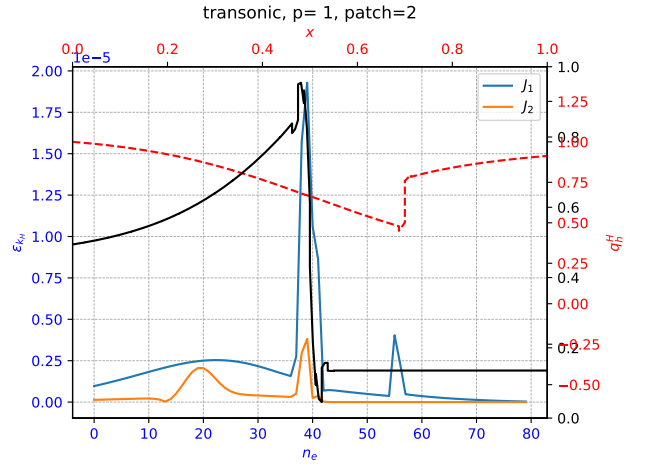


(b) Effectivity with $p_H = 2$ on \mathcal{M}_H for J_2

Figure 11: Effectivity for J_2 in the transonic regime.

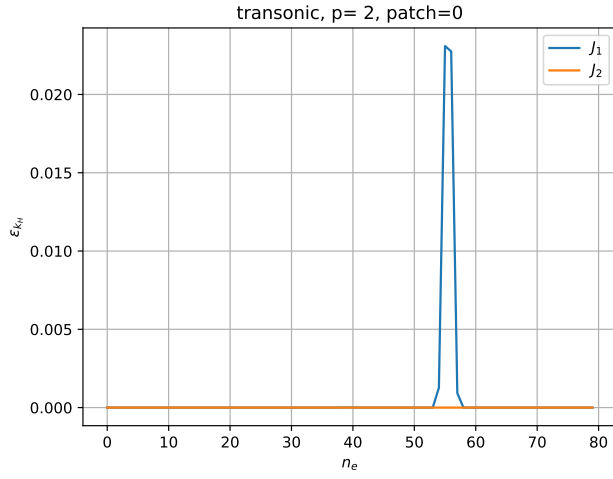


(a)

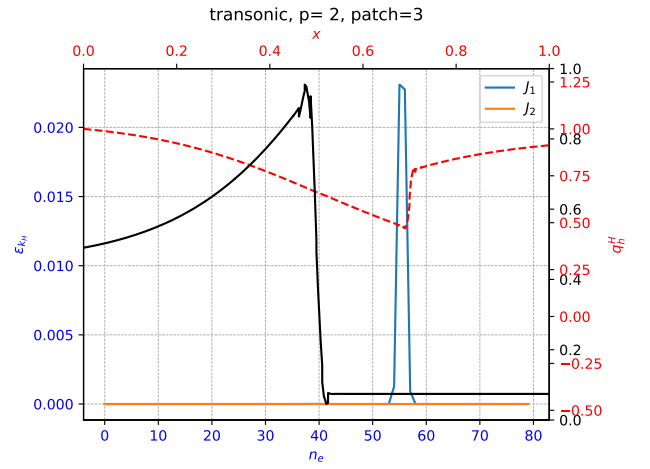


(b)

Figure 12: AWR based mesh refinement prediction in the transonic regime for $p_H = 1$.



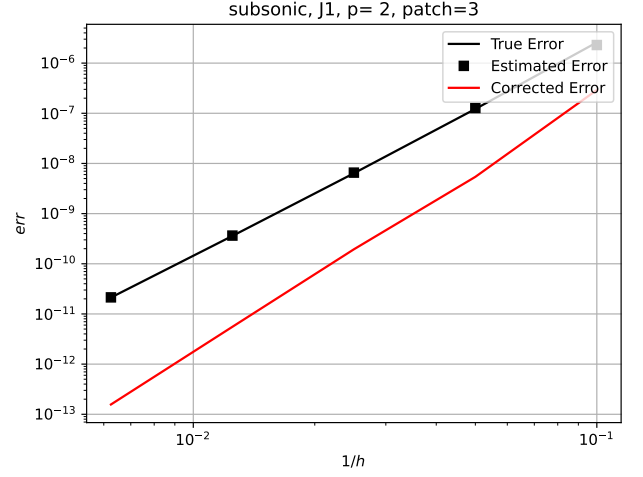
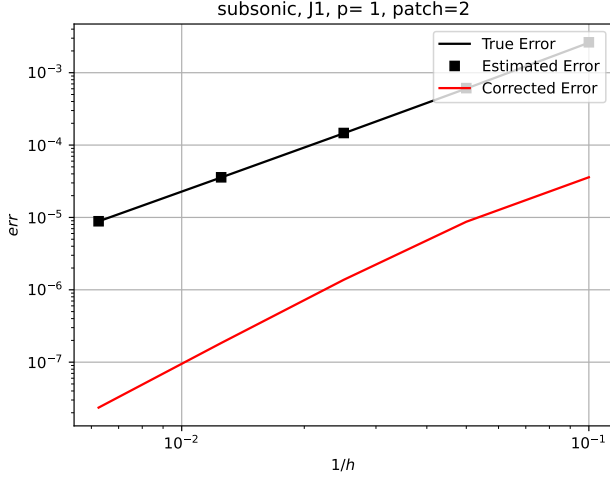
(a)



(b)

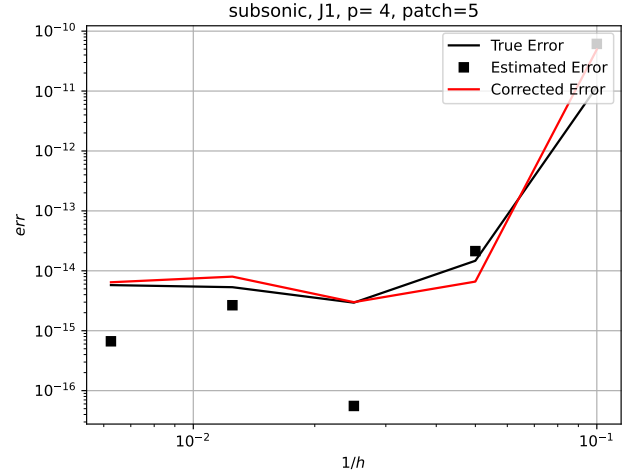
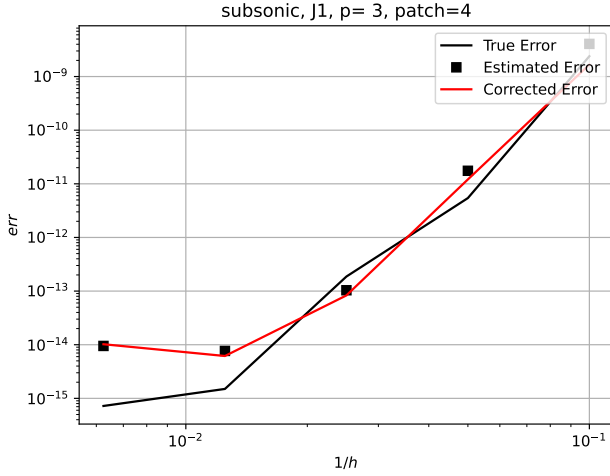
Figure 13: AWR based mesh refinement prediction in the transonic regime for $p_H = 2$.

A Subsonic - patch reconstruction



(a) Error convergence with patching on $p_H = 1$ on \mathcal{M}_H for J_1

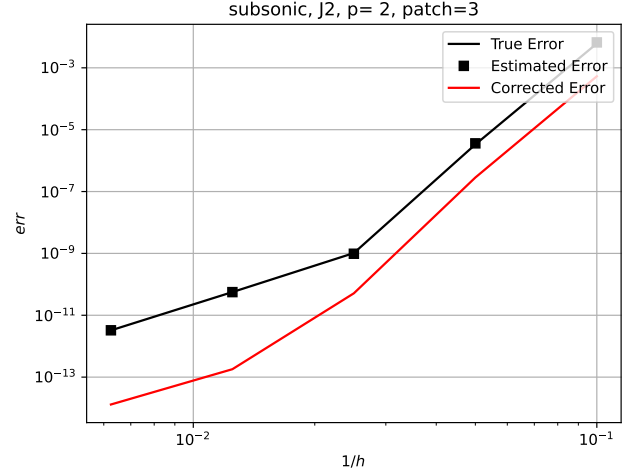
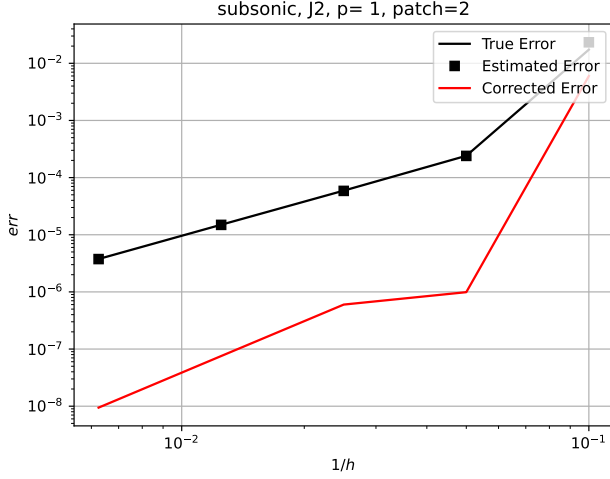
(b) Error convergence with patching on $p_H = 2$ on \mathcal{M}_H for J_1



(c) Error convergence with patching on $p_H = 3$ on \mathcal{M}_H for J_1

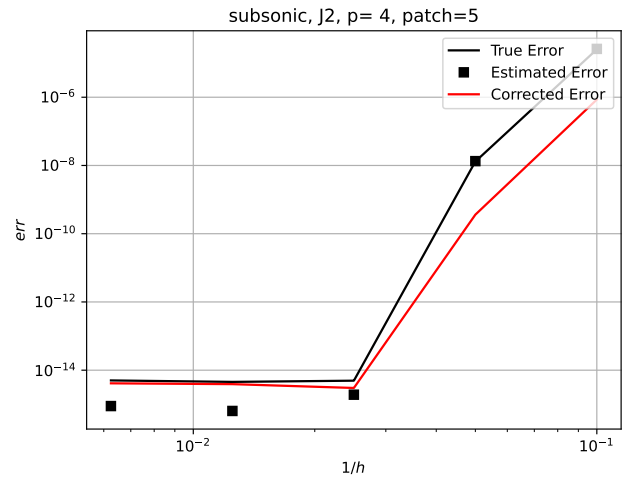
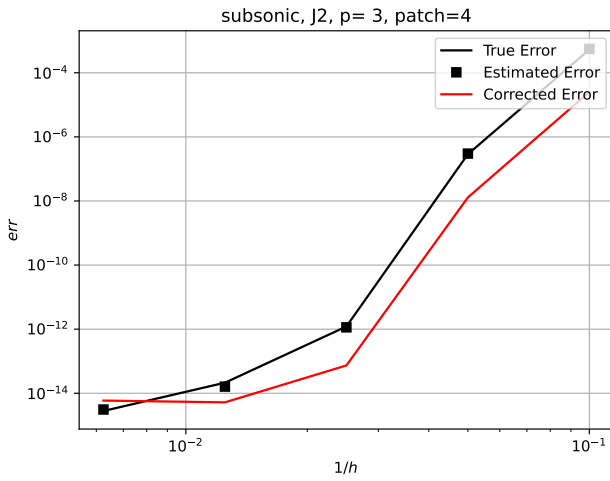
(d) Error convergence with patching on $p_H = 4$ on \mathcal{M}_H for J_1

Figure A.1: Mesh convergence analysis for functional J_1 using AWR showing the true error, estimated error and the corrected error in the subsonic flow regime with patching.



(a) Error convergence with patching on $p_H = 1$ on \mathcal{M}_H for J_2

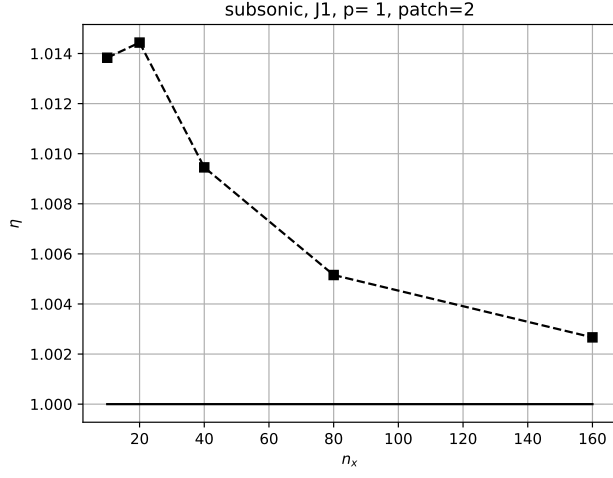
(b) Error convergence with patching on $p_H = 2$ on \mathcal{M}_H for J_2



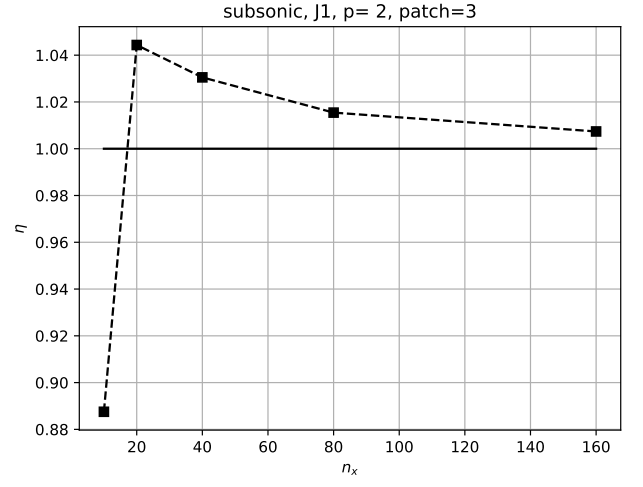
(c) Error convergence with patching on $p_H = 3$ on \mathcal{M}_H for J_2

(d) Error convergence with patching on $p_H = 4$ on \mathcal{M}_H for J_2

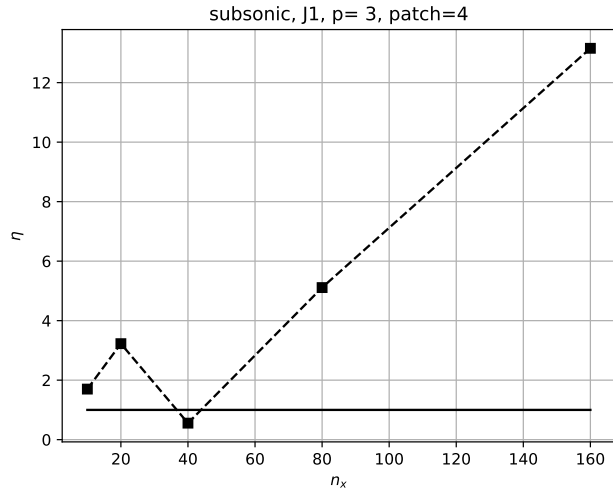
Figure A.2: Mesh convergence analysis for functional J_2 using AWR showing the true error, estimated error and the corrected error in the subsonic flow regime with patching.



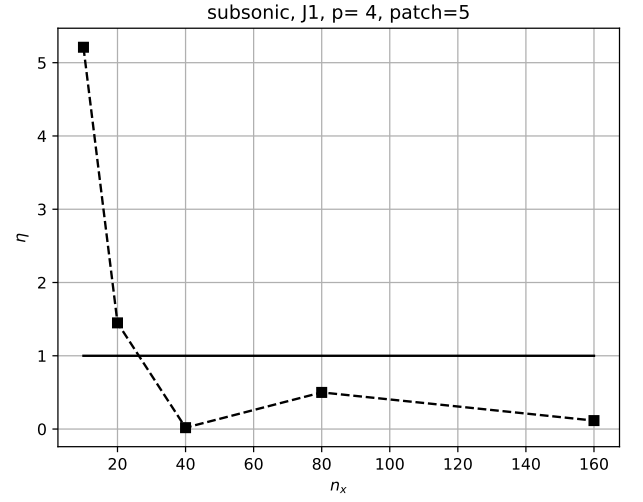
(a) Effectivity with $p_H = 1$ on \mathcal{M}_H for J_1



(b) Effectivity with $p_H = 1$ on \mathcal{M}_H for J_1

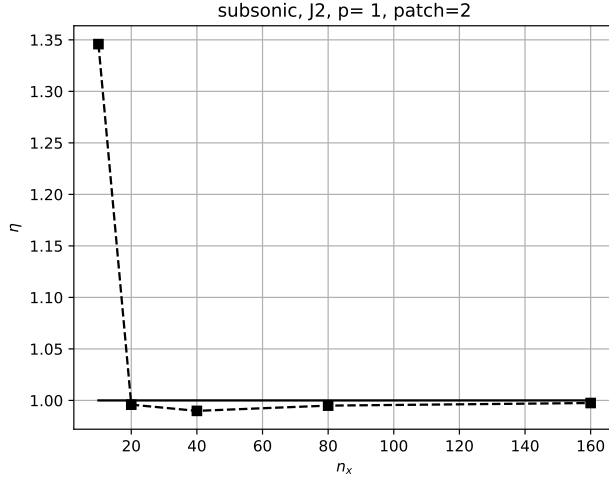


(c) Effectivity with $p_H = 1$ on \mathcal{M}_H for J_1

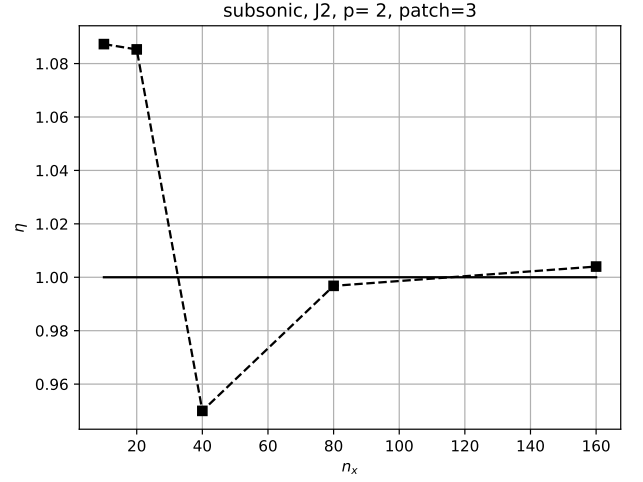


(d) Effectivity with $p_H = 1$ on \mathcal{M}_H for J_1

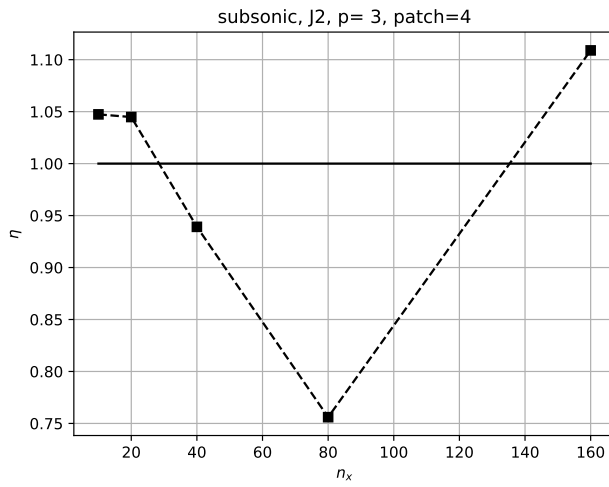
Figure A.3: Effectivity for J_1 in the subsonic flow regime with patching.



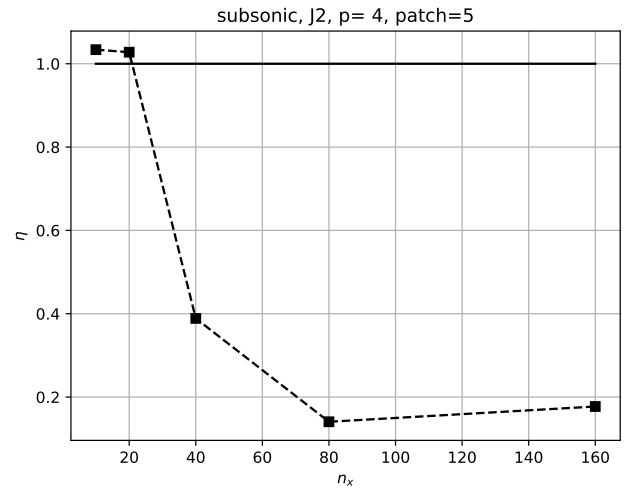
(a) Effectivity with $p_H = 1$ on \mathcal{M}_H for J_2



(b) Effectivity with $p_H = 1$ on \mathcal{M}_H for J_2



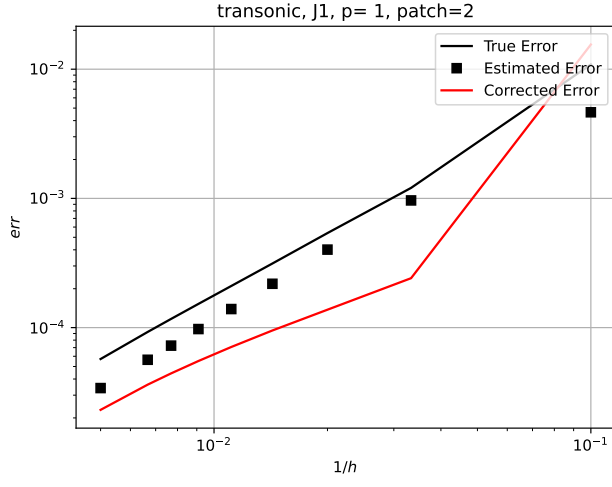
(c) Effectivity with $p_H = 1$ on \mathcal{M}_H for J_2



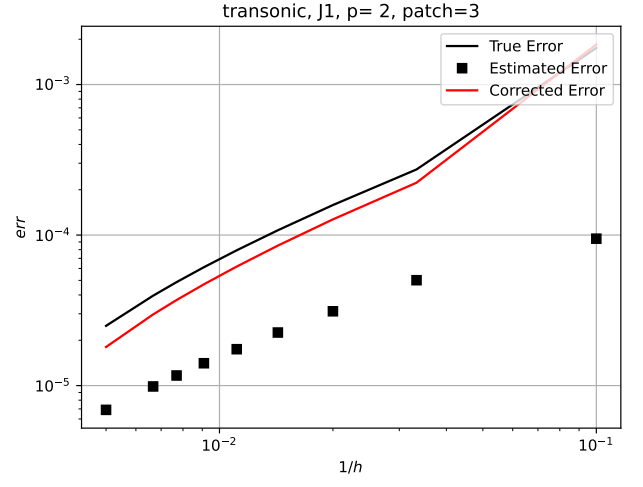
(d) Effectivity with $p_H = 1$ on \mathcal{M}_H for J_2

Figure A.4: Effectivity for J_2 in the subsonic flow regime with patching.

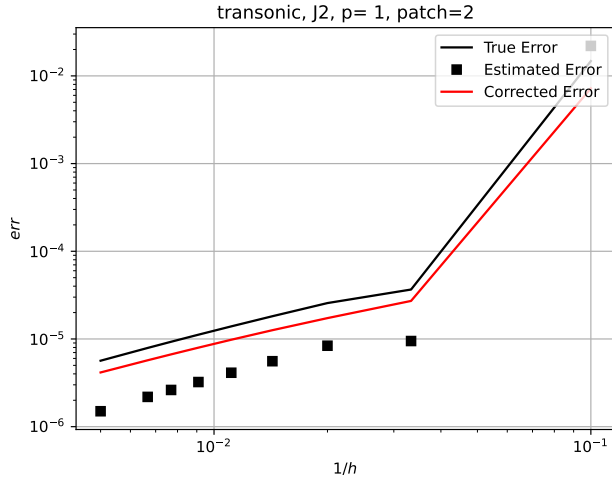
B Transonic - patch reconstruction



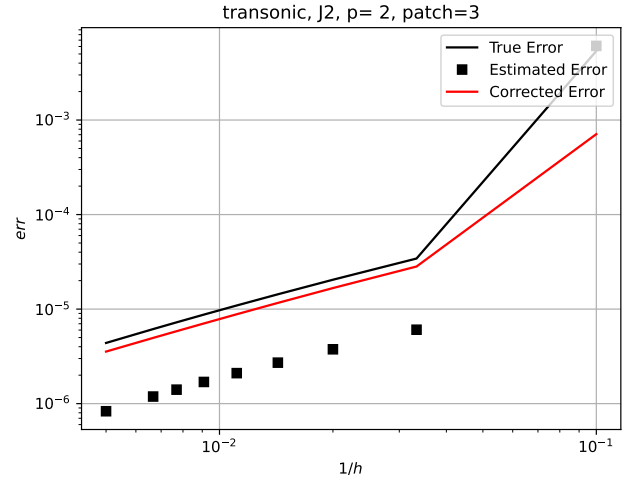
(a) Error convergence on $p_H = 1$ on \mathcal{M}_H for J_1



(b) Error convergence on $p_H = 2$ on \mathcal{M}_H for J_1

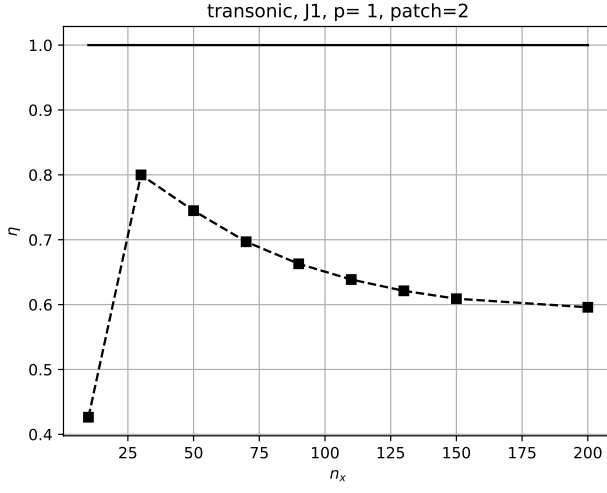


(c) Error convergence on $p_H = 1$ on \mathcal{M}_H for J_2

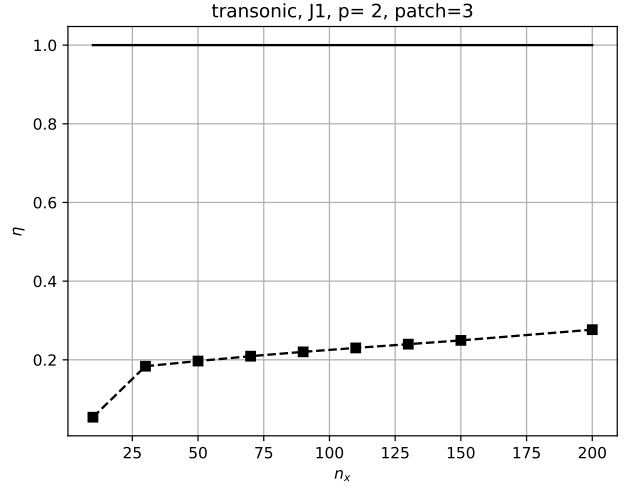


(d) Error convergence on $p_H = 2$ on \mathcal{M}_H for J_2

Figure B.1: Mesh convergence analysis for functional J_1, J_2 using AWR showing the true error, estimated error and the corrected error in the transonic flow regime with patching.

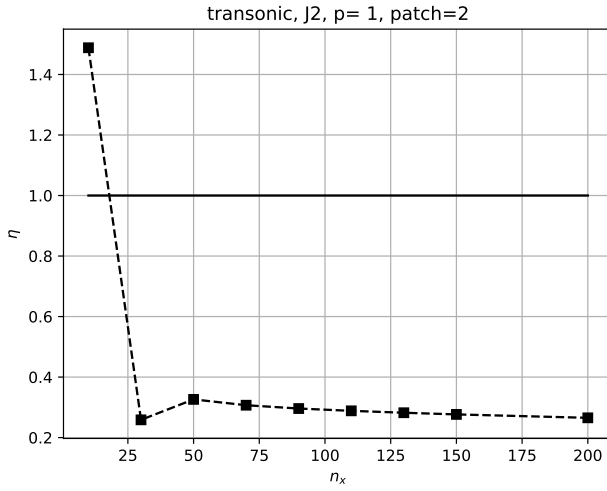


(a) Effectivity with $p_H = 1$ on \mathcal{M}_H for J_1

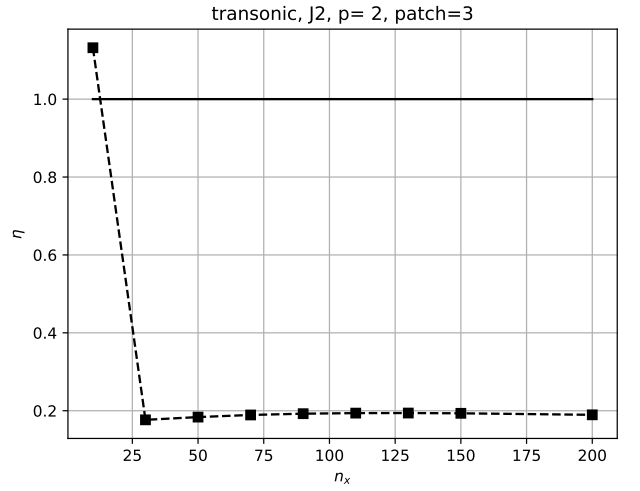


(b) Effectivity with $p_H = 2$ on \mathcal{M}_H for J_1

Figure B.2: Effectivity for J_1 in the transonic regime with patching.



(a) Effectivity with $p_H = 1$ on \mathcal{M}_H for J_2



(b) Effectivity with $p_H = 2$ on \mathcal{M}_H for J_2

Figure B.3: Effectivity for J_2 in the transonic regime with patching.